GEOSCIENCE FRONTIERS 3(5) (2012) 635–646

available at www.sciencedirect.com

China University of Geosciences (Beijing)

GEOSCIENCE FRONTIERS

journal homepage: www.elsevier.com/locate/gsf

RESEARCH PAPER

An Early Cretaceous garnet-bearing metaluminous A-type granite intrusion in the East Qinling Orogen, central China: Petrological, mineralogical and geochemical constraints

Jinyang Zhang [a,*], Changqian Ma [b,c], Zhenbing She [b]

[a] *Faculty of Earth Resources, China University of Geosciences, Wuhan 430074, China*
[b] *Faculty of Earth Sciences, China University of Geosciences, Wuhan 430074, China*
[c] *State Key Laboratory of Geological Processes and Mineral Resources, China University of Geosciences, Wuhan 430074, China*

Received 30 June 2011; accepted 16 November 2011
Available online 17 February 2012

KEYWORDS
Garnet;
A-type granite;
Early Cretaceous;
East Qinling Orogen

Abstract The Erlangmiao granite intrusion is located in the eastern part of the East Qinling Orogen. The granite contains almost 99 vol.% felsic minerals with accessory garnet, muscovite, biotite, zircon, and Fe-Ti oxide. Garnet is the dominant accessory mineral, shows zoned texture, and is rich in w(FeO) (14.13%–16.09%) and w(MnO) (24.21%–27.44%). The rocks have high SiO_2, alkalis, FeO_t/MgO, TiO_2/MgO and low Al_2O_3, CaO with $w(Na_2O)/w(K_2O) > 1$. Their Rb, Ga, Ta, Nb, Y, and Yb contents are high and Sr, Ba, Eu, Zr, P, and Ti contents are low. These features indicate that the Erlangmiao granite is a highly evolved metaluminous A-type. Garnet crystallized at the expense of biotite from the MnO-rich evolved melt after fractionation of biotite, plagioclase, K-feldspar, zircon, apatite, and ilmenite. The relatively high initial $^{87}Sr/^{86}Sr$ ratios (0.706–0.708), low and negative ε_{Nd} (120 Ma) values

* Corresponding author. Faculty of Earth Resources, China University of Geosciences, No. 388, Lumo Road, Wuhan 430074, China.
E-mail addresses: geomantleflow@gmail.com, zhangjinyang@cug.edu.cn (J. Zhang).

Peer-review under responsibility of China University of Geosciences (Beijing).
doi:10.1016/j.gsf.2011.11.011

Production and hosting by Elsevier

(−6.6 to −9.0), and old Nd model ages (1.5–1.7 Ga) suggest that the rocks were probably formed by partial melting of the Paleoproterozoic granitic gneisses from the basement, with participation of depleted mantle in an extensional setting.

1. Introduction

Garnet-bearing granites are widely distributed in orogenic belts (Barbarin, 1996, 1999; Sylvester, 1998) and their genesis is still controversial. The vast majority of garnet-bearing granites are S-type and were probably derived from partial melting of predominantly metasedimentary crustal rocks (Chappell and White, 1974; Clemens, 2003) although a few authors have questioned the whole concept of S-type granites (e.g. Kemp et al., 2007). A minority of garnet-bearing granites have more complicated origins than ordinary S-type granites. Some are I-type granites that have undergone unusual fractionation or contamination in volcanic arcs (White et al., 1986; du Bray, 1988; Zhou and Yu, 2001; Wu et al., 2004; Yu et al., 2004), whereas others are A-type granites formed in anorogenic or extensional environments (du Bray, 1988).

Garnet is an uncommon constituent within granite and has variable compositions. It has been shown that spessartine-rich garnet generally crystallized in equilibrium with S-type, aluminum- and manganese-rich granitic magma at relative low pressures (Green, 1977; Abbott, 1981; Allan and Clarke, 1981; Stone, 1988; Dahlquist et al., 2007). However, du Bray (1988) argued that a manganese-rich condition is probably not required for crystallization of spessartine-rich garnet. It is undetermined whether there is a relationship between garnet composition and granite genesis and what controls garnet crystallization from granite (Miller and Stoddard, 1981; Stevens et al., 2007; Villaros et al., 2009).

The eastern part of the East Qinling Orogen, central China, contains large volumes of Early Cretaceous granites (Li et al., 1993), and the majority of them are I-types. However, a garnet-bearing A-type granite intrusion occurs at the Erlangmiao and thus provides an opportunity to discuss garnet genesis and petrogenesis.

2. Geological setting

The Qinling Orogen extends for over 2000 km across central China, separating the North China Craton to the north from the Yangtze Craton to the south (Fig. 1a). It has a prolonged Precambrian history (Zhang et al., 1996; Zhu et al., 2011) and was mainly built by two collisional events during Early–Middle Paleozoic and Early Mesozoic and the Shangdan and Mianlue suture zones formed during these collisions (Ratschbacher et al., 2003; S.Z. Li et al., 2007; Tseng et al., 2009; Xiang et al., 2011). Geographically, it is commonly separated into a western

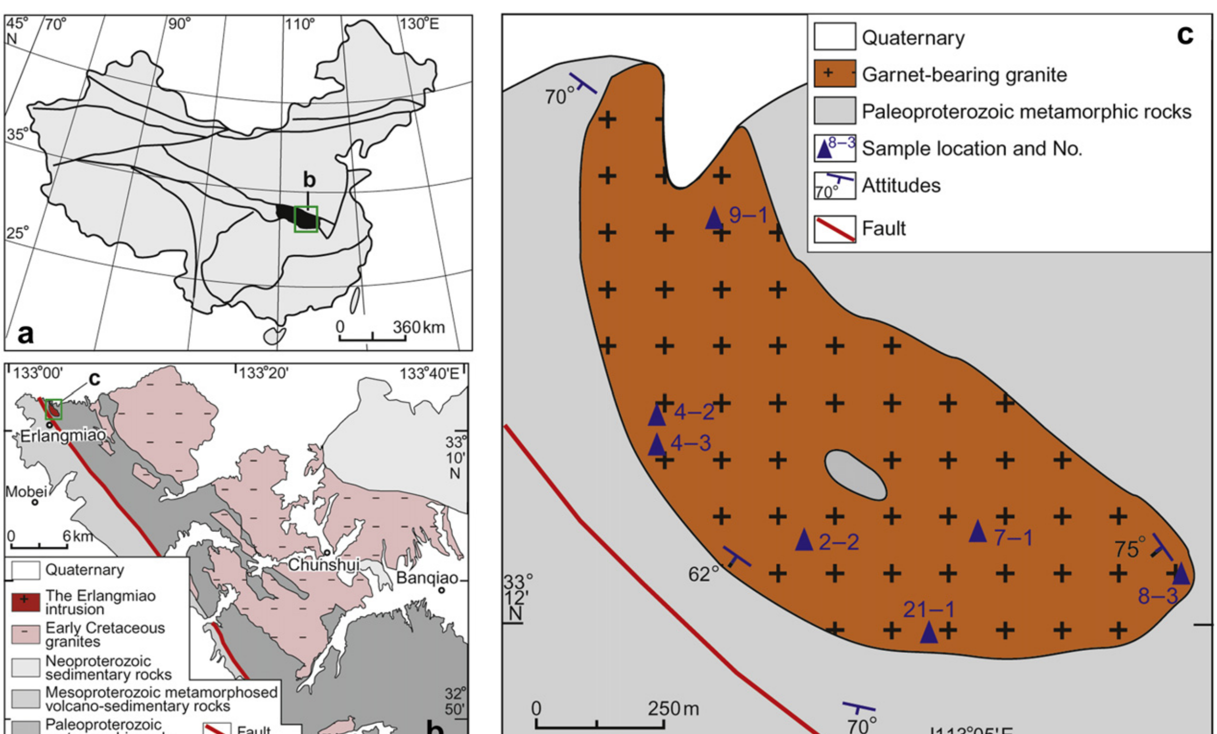

Figure 1 a: Simplified map of China. Black area represents the East Qinling Orogen; b: Geological map of the eastern portion of East Qinling Orogen; c: Simplified geological map of the Erlangmiao intrusion showing sample locations. A roof pendant is shown within the intrusion. 2-2, abbreviation for 05HL02-2.

and an eastern orogen. Our study area is located in the eastern part of the East Qinling Orogen and consists mainly of Paleoproterozoic metamorphic rocks, Mesoproterozoic metamorphosed volcano-sedimentary rocks, Neoproterozoic sedimentary rocks and Early Cretaceous granites (BGMRHP, 1989) (Fig. 1b). The Paleoproterozoic metamorphic rocks are strongly migmatitic and their protoliths are difficult to be distinguished. Detailed field surveys and petrographical studies indicate that they are mainly composed of banded, augen migmatites and migmatitic gneisses and were mainly undergone Neoproterozoic and Early Cretaceous migmatization (BGMRHP, 1989). The Mesoproterozoic metamorphosed volcano-sedimentary rocks are composed chiefly of amphibolite- to greenschist-facies two-mica quartz schists and marbles. Zircon U-Pb geochronological studies from the Shangzhou in Shanxi Province indicate that their protoliths were formed during 1150–1200 Ma and then metamorphosed at 1100 Ma (Zhang et al., 2004a). The Neoproterozoic sedimentary rocks are sandstones and pelites and were deposited as coastal and neritic facies (BGMRHP, 1989).

The Early Cretaceous granites are mainly biotite monzogranite and were emplaced at 120–130 Ma based on dating by the LA-ICP-MS zircon U-Pb method (Zhou et al., 2008). The Erlangmiao intrusion was emplaced later than the other widespread Early Cretaceous granites in the region and contains garnet that is visible in the field, which is the only garnet-bearing intrusive body in the region.

3. Field occurrence of the Erlangmiao granite

The Erlangmiao intrusion is located in the eastern part of Fangcheng County, Henan Province and has an elliptical shape and an exposure of ca. 1.5 km^2 (Fig. 1c). It intruded migmatitic gneisses with sharp contacts, and was itself intruded by fine-grained aplites and coarse-grained pegmatites. The intrusion includes medium- and fine-grained granite. The medium-grained granite constitutes the main body of the intrusion and the fine-grained granite only occurs in the southeast margin of the intrusion, where it is several tens of meters wide and has a transitional relationship with medium-grained granite and sharp contacts with the migmatitic gneiss. Large roof pendants of migmatitic gneiss are found within the intrusion. Garnet can be observed randomly throughout the intrusion and forms aggregates (Fig. 2a) in the northwest of the intrusion. Migmatitic gneiss xenoliths, chilled margins of 10 cm wide, and biotite schist xenoliths occur at the southeast margin of the intrusion (Fig. 2b). The angular xenoliths and chilled margins within the Erlangmiao intrusion suggest that the granite was emplaced at a shallow crustal level.

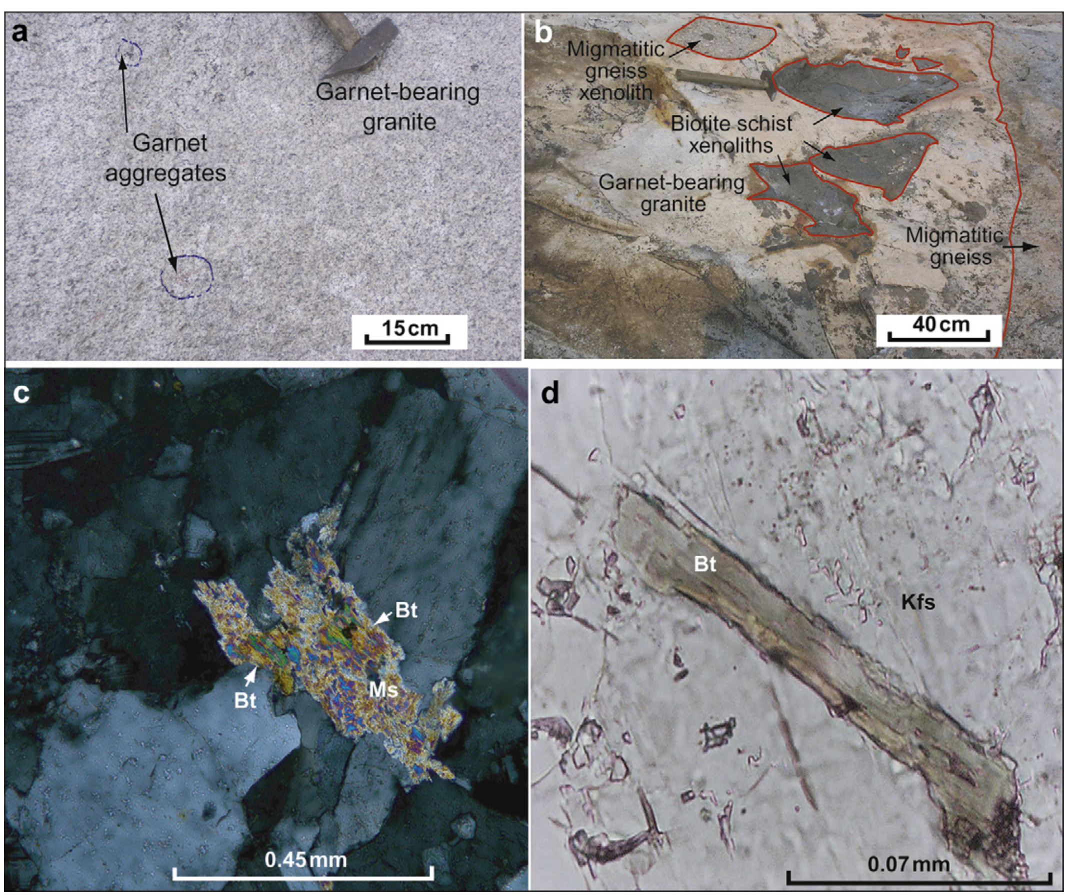

Figure 2 a: Garnet-bearing granite containing garnet aggregates from the northwest part of the Erlangmiao intrusion; b: Migmatitic gneiss and biotite schist xenoliths in the southeast margin of the Erlangmiao intrusion; c: Biotite (Bt) and muscovite (Ms) aggregate from sample 05HL08-3 in cross-polarized light; d: An acicular biotite crystal among K-feldspar (Kfs) crystals from sample 05HL08-3 in plane-polarized light.

4. Petrographic description of the Erlangmiao granite

The Erlangmiao granite contains quartz (∼34 Vol.%), K-feldspar (∼40 Vol.%), plagioclase (∼25 Vol.%), and accessory minerals (1 Vol.%−2 Vol.%). Accessory minerals include garnet, muscovite, biotite, zircon, and Fe-Ti oxide. Plagioclase is usually euhedral and few sericite aggregates occur along cleavages and at the edges of grains. K-feldspar includes microcline and mesoperthite. Quartz forms typically interstitial anhedral grains with undulose extinction. Brownish yellow, subhedral to euhedral garnet crystals, with diameters of about 1−1.5 mm and containing irregular cracks, form a dominant proportion of the accessory minerals and are ubiquitous within the intrusion. They are locally zoned, with large, brownish yellow cores and thin, colorless rims. The resorbed (as showed in Fig. 3) rims of garnet were observed. The contents of biotite and muscovite are low. They are commonly altered and occasionally form aggregates (Fig. 2c). Some acicular biotite grains are distributed among K-feldspar (Fig. 2d). Euhedral zircon crystals within plagioclase were observed. Undulose extinction, subgrain and polygonal grain of quartz, curving micas, porphyroclastic feldspar, and sericite appear and occur more frequently near the southwest of the Erlangmiao intrusion, which confirms that deformation overprinting granitic rocks is stronger near the southwest contact zone.

5. Analytic methods

Major elements in garnet were analyzed at the State Key Laboratory of Geological Processes and Mineral Resources at China University of Geosciences (Wuhan) using a JEOL JXA-8100 electron microprobe, with an accelerating voltage of 15 kV and a sample current of 15 nA. The beam diameter was 2 μm. Errors in the major oxides are estimated to be less than 3%. Garnet compositions were recast to end-members using the Minpet software of Linda R. Richard. End-members were calculated following Deer et al. (1992), while Fe^{3+} determined and followed Droop (1987). Crystal chemical formulas were based on 12 oxygens and 8 cations.

Whole-rock samples were crushed in a steel crusher and powdered to 200-mesh size using an agate mill. Major and trace elements were measured at the Hubei Institute of Experimental Geology in Wuhan, Hubei Province. H_2O^+ was determined by gravimetry, CO_2 by volumetry, and other major elements by X-Ray Fluorescence (XRF). Relative standard derivations (RSD) are within 1% except for H_2O^+ and CO_2. Rare earth elements, Y, Ba, Co, Ni, Sr, V, Nb, Ta, Zr, Hf, Sc, and Th were determined by Inductively Coupled Plasma Atomic Emission Spectroscopy (ICP-AES); Rb, Pb, and Cr by XRF; Ga by Powder Emission Spectrometry (PES); and U by Laser Induced Fluorescence Spectroscopy (LIFS) with RSD of 3%−10%. Analyses of

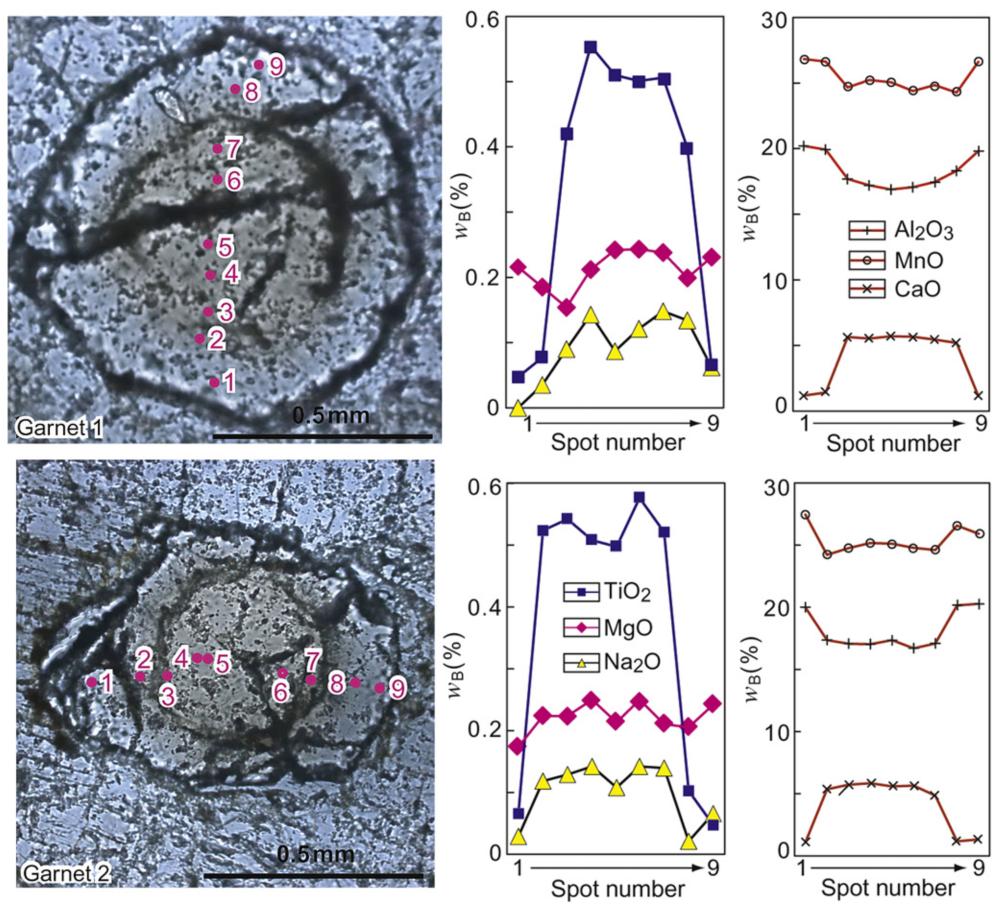

Figure 3 Microphotographs (plane-polarized light) and compositions of zoned garnet from the Erlangmiao granite. Solid circles and numbers represent analytical spots and their symbols.

international standard reference samples and details of apparatus were reported in Gao et al. (1991). Sr-Nd isotopic analyses were determined using a MAT-262 at the Institute of Geology and Geophysics, Chinese Academy of Sciences (CAS), Beijing, following procedures described by Chen et al. (2000).

6. Garnet chemistry

The results of major element analysis of two zoned garnet grains from the Erlangmiao granite (05HL04-3) are listed in Table 1. The garnet is MnO-rich and MgO-poor. The rims of both grains contain lower CaO and TiO_2 contents but higher MnO and Al_2O_3 contents than the cores. Distribution of MgO, FeO, and Na_2O contents is relatively complex between the rims and the cores (Fig. 3). The cores of garnet are mainly composed of spessartine (~ 54 mol.%), almandine (~ 30 mol.%), and grossular (~ 12 mol.%) with small amounts of andradite (~ 3 mol.%) and pyrope (~ 1 mol.%), while the rims are dominated by spessartine (~ 62 mol.%) and almandine (~ 34 mol.%) with few andradite (~ 3 mol.%), pyrope (~ 1 mol.%), and grossular (~ 1 mol.%).

7. Whole rock geochemistry

The results of major oxides, trace elements, and Sr-Nd isotope analyses of the Erlangmiao granite are given in Tables 2 and 3. The granite has high SiO_2 and alkalis contents, and very low CaO, FeO, Fe_2O_3, and MgO contents, with $w(K_2O)/w(Na_2O) < 1$. Most samples show metaluminous character with ACNK molar Al_2O_3/($CaO+Na_2O+K_2O$) < 1; only two samples exhibit higher ACNK values (1.03−1.05) and are weakly peraluminous. The rocks are characterized by low total rare earth element (REE) contents and light REE (LREE)/heavy REE (HREE) ratios (8.6−9.8) with a strong negative Eu anomaly. The primitive mantle-normalized REE patterns are slope to the left (Fig. 4a), influencing obviously by garnet. Three samples show slight tetrad effects with TE1, 3 ≤ 1 (Wu et al., 2004). Rubidium, K, Th, Ta, Nb, Zr, Hf, Y, and Yb contents of the rocks are high while Ba, Ce, and Sm contents are low on primitive mantle-normalized spider diagrams (Fig. 4b). Al_2O_3, Fe_2O_3, Na_2O, K_2O, and Rb contents decrease, while MgO and MnO contents increase with variation in SiO_2 (Fig. 5). Calculated initial Sr isotopic ratios (I_{Sr}) vary from 0.706 to 0.708 and ε_{Nd} (120 Ma) from −6.6 to −9.0. We calculated Nd model ages using a two-stage evolutionary model (t_{2DM}) (Li, 1996) because the $^{147}Sm/^{144}Nd$ ratios are larger than that of average crust (0.12). Neodymium model ages are 1.5−1.7 Ga.

8. Discussion

Chemical changes influenced by deformation should be identified and excluded. Mylonite deformation has little influence on Nd isotopic compositions but strongly affects Sr isotopic systematics (Barovich and Patchett, 1992). The effect of mylonite deformation on major and trace elements is rather complex and different results have been attained (Kerrich et al., 1980; Bialek, 1999). Appearance of sericite, undulose extinction of quartz, and porphyroclastic feldspar in thin sections are more readily present within samples 05HL04-2 and 05HL04-3, together with their abnormal $^{87}Rb/^{86}Sr$ and I_{Sr} ratios, evidencing the effect of deformation. Therefore, I_{Sr} values were obviously influenced by deformation, while most elements and Nd isotopes changed little and it is feasible to use data of most elements and Nd isotopes to discuss petrogenesis of the Erlangmiao granite.

8.1. Garnet genesis

Garnet could occur: (1) as a refractory restite phase (René and Stelling, 2007) or peritectic entrainment from the zone of partial melting (Stevens et al., 2007); (2) as a xenocryst from upper mantle rocks and/or crustal metamorphic rocks (Embey-Isztin et al., 1985); (3) as a low-pressure precipitate or high-pressure phenocryst from melt (René and Stelling, 2007). Magmatic garnet in igneous rocks can be classified into three groups: (1) it occurs in strongly

Table 1 Compositions of representative zoned garnet from sample 05HL04-3 of the Erlangmiao granite.

	Grain 1									Grain 2								
	Gt1-1	Gt1-2	Gt1-3	Gt1-4	Gt1-5	Gt1-6	Gt1-7	Gt1-8	Gt1-9	Gt2-1	Gt2-2	Gt2-3	Gt2-4	Gt2-5	Gt2-6	Gt2-7	Gt2-8	Gt2-9
	Rim	Rim	Core	Core	Core	Core	Core	Core	Rim	Rim	Core	Core	Core	Core	Core	Core	Rim	Rim
SiO_2	36.17	36.10	35.94	35.91	36.16	36.67	35.80	35.90	36.18	36.08	35.98	36.85	36.38	36.10	36.62	36.42	36.29	36.22
TiO_2	0.05	0.08	0.42	0.56	0.51	0.50	0.51	0.40	0.06	0.07	0.52	0.54	0.51	0.50	0.58	0.52	0.10	0.05
Al_2O_3	20.21	19.92	17.68	17.19	16.89	17.06	17.45	18.32	19.82	19.99	17.36	17.06	17.03	17.36	16.70	17.08	20.15	20.29
FeO	15.40	15.65	14.80	14.70	14.68	15.09	14.78	14.81	15.42	15.38	15.73	14.84	14.83	14.13	15.40	16.09	15.31	15.99
MnO	26.82	26.64	24.66	25.22	25.06	24.40	24.84	24.27	26.62	27.44	24.21	24.77	25.17	25.11	24.78	24.60	26.57	25.90
MgO	0.22	0.19	0.15	0.21	0.24	0.24	0.24	0.20	0.23	0.17	0.23	0.23	0.25	0.21	0.25	0.21	0.21	0.24
CaO	1.19	1.42	5.65	5.54	5.71	5.68	5.45	5.21	1.16	1.09	5.36	5.73	5.84	5.60	5.66	4.85	1.18	1.33
Na_2O	−	0.04	0.09	0.14	0.09	0.12	0.15	0.13	0.06	0.03	0.12	0.13	0.14	0.11	0.14	0.14	0.02	0.07
K_2O	0.00	0.03	0.01	0.00	0.01	0.02	0.02	0.01	0.01	−	0.01	0.01	−	0.02	0.01	0.03	−	0.02
Cr_2O_3	0.01	0.03	−	0.02	−	−	−	0.00	0.01	0.00	−	−	0.01	−	0.02	0.04	−	0.01
Total	100.06	100.08	99.40	99.49	99.35	99.78	99.23	99.25	99.58	100.26	99.52	100.15	100.16	99.13	100.15	99.98	99.82	100.11
Spess	62.2	61.3	53.7	54.4	53.9	52.9	54.0	53.8	62.0	63.0	52.4	53.5	53.7	54.8	52.9	53.3	62.1	60.2
Alm	33.5	33.8	30.2	29.7	29.6	30.7	30.1	30.8	33.7	33.1	32.0	30.0	29.7	28.9	30.9	32.7	33.6	34.9
And	2.7	2.7	2.9	2.9	2.9	3.0	2.9	2.8	2.7	2.7	3.1	2.9	2.9	2.8	3.2	3.2	2.6	2.7
Gross	0.8	1.4	12.7	12.2	12.6	12.6	12.1	11.8	0.7	0.5	11.6	12.7	12.8	12.7	12.1	10.1	0.9	1.2
Pyrope	0.9	0.8	0.6	0.8	0.9	0.9	0.9	0.8	0.9	0.7	0.9	0.9	0.9	0.8	0.9	0.8	0.8	1.0

Gt, garnet; −, not detected.

Table 2 Representative major and trace element analysis of the Erlangmiao garnet-bearing granite.

Samples	05HL02-2	05HL04-2	05HL04-3	05HL07-1	05HL08-3	05HL09-1	05DB21-1
SiO_2	77.39	75.03	75.98	76.94	76.64	76.38	77.28
TiO_2	0.05	0.05	0.10	0.04	0.04	0.06	0.05
Al_2O_3	12.46	13.66	13.09	12.55	12.86	12.91	12.90
Fe_2O_3	0.21	0.47	0.74	0.42	0.32	0.42	0.25
FeO	0.28	0.22	0.1	0.17	0.13	0.13	0.13
MnO	0.07	0.12	0.15	0.20	0.17	0.03	0.26
MgO	0.20	0.10	0.06	0.15	0.12	0.13	0.08
CaO	0.77	0.77	0.37	0.49	0.57	0.71	0.86
Na_2O	4.51	4.82	4.68	4.63	5.18	4.24	4.28
K_2O	3.49	4.21	3.99	3.89	3.51	4.57	3.44
P_2O_5	0.03	0.02	0.03	0.03	0.05	0.02	0.02
CO_2	0.04	0.04	0.04	0.04	0.02	0.04	0.06
H_2O^+	0.37	0.38	0.53	0.36	0.26	0.26	0.28
Total	99.87	99.89	99.86	99.91	99.87	99.90	99.89
Cr	4.80	6.10	4.30	6.00	6.00	4.50	4.30
Sc	6.70	13.0	17.0	7.60	11.0	2.70	8.80
V	3.10	4.80	2.80	5.90	7.80	3.80	6.10
Ga	25.3	30.9	34.8	39.9	34.5	23.5	26.9
Rb	326	464	477	408	357	340	264
Sr	13.2	9.20	4.00	3.20	60.2	10.6	10.1
Y	20.4	39.6	31.6	50.2	23.1	10.9	89.2
Nb	42.4	81.1	109	77.2	94.8	29.6	36.9
Zr	56.6	113	92.6	116	108	50.2	58.3
Ba	7.90	10.7	14.6	9.20	74.8	15.4	11.7
Hf	4.20	7.70	6.90	7.20	6.90	3.80	2.40
Ta	4.90	6.20	6.50	4.50	8.90	2.20	2.10
Pb	41.3	63.8	58.4	47.6	50.2	42.6	33.9
Th	15.0	18.8	21.8	26.2	8.42	19.0	16.6
U	11.7	17.6	26.5	25.0	2.78	6.47	13.0
La	2.87	1.53	2.57	0.97	2.49	3.30	1.46
Ce	5.15	3.19	6.13	2.33	3.33	4.81	2.69
Pr	0.77	0.55	0.89	0.38	0.60	0.87	0.47
Nd	3.16	3.00	3.58	1.66	2.11	3.15	2.35
Sm	1.04	1.34	1.25	1.02	0.55	0.79	1.17
Eu	0.07	0.05	0.05	0.05	0.07	0.09	0.07
Gd	1.15	1.80	1.66	1.58	0.70	0.84	2.18
Tb	0.25	0.45	0.42	0.47	0.19	0.19	0.62
Dy	1.82	3.54	3.24	4.10	1.52	1.29	6.79
Ho	0.49	0.97	0.91	1.16	0.35	0.32	2.34
Er	1.99	3.87	3.58	4.95	1.20	1.22	12.2
Tm	0.42	0.86	0.77	1.15	0.27	0.24	3.18
Yb	3.54	7.52	6.33	10.2	2.11	1.91	33.0
Lu	0.65	1.39	1.14	1.89	0.35	0.34	6.80

peraluminous S-type dacites-rhyolites or granites and crystallized under low pressure in the upper crust with high FeO contents (w(FeO) > 30%) (Clemens and Wall, 1981, 1984; Gilbert and Rogers, 1989; Lackey et al., 2006; René and Stelling, 2007; Mirnejad et al., 2008); (2) occurs in basalts, andesites, dacites, rhyolites or tonalitic and granodioritic porphyries and crystallized under high pressure in the lower crust or mantle with w(FeO) 20%–30%, w(MgO) 5%–10%, and w(CaO) ~5% (Green and Ringwood, 1968; Hamer and Moyes, 1982; Day et al., 1992; Harangi et al., 2001; Aydar and Gourgaud, 2002; Patranabis-Deb et al., 2009; Yuan et al., 2009); and (3) occurs in pegmatites, aplites, and granites and crystallized from post-magmatic fluids or highly fractionated magma with w(MnO) ~30% and w(FeO) 10%–15% (Speer and Becker, 1992; Whitworth, 1992). The Erlangmiao garnet is euhedral to subhedral, strongly zoned, and has high FeO and MnO contents. It is magmatic origin and crystallized from highly fractionated granite.

Miller and Stoddard (1981) and Abbott (1981) discussed and reviewed how garnet could crystallize at the expense of biotite in MnO- and Al_2O_3-rich evolved magma. However, Hogan (1996) argued that late crystallization of garnet reflects increasing Al in the melt but does not necessarily require high Mn activities for the melt. Positive relationship of SiO_2 and MnO, rather higher w(MnO)/w(FeO_t + MgO) ratios (0.1–0.5) of the Erlangmiao granite, and MnO-rich garnet support that the Erlangmiao granite crystallized from a highly evolved MnO-rich magma. The Erlangmiao granite

Table 3 Representative Sr-Nd isotopic data of the Erlangmiao garnet-bearing granite.

Samples	05HL04-3	05HL07-1	05HL09-1	05DB21-1	05HL08-3
Rb	505	421	361	279	370
Sr	3.64	2.84	9.89	8.72	49.6
$^{87}Rb/^{86}Sr$	430.3	454.9	107.5	93.18	21.43
$^{87}Sr/^{86}Sr$	1.386541	1.417543	0.876193	0.852025	0.740663
2σ	0.000036	0.000082	0.000049	0.000012	0.000012
I_{Sr}	0.713949	0.706488	0.708087	0.706366	0.707164
Sm	1.43	0.956	0.846	1.14	0.578
Nd	4.07	1.54	3.40	2.21	2.09
$^{147}Sm/^{144}Nd$	0.2123	0.3740	0.1503	0.3120	0.1671
$^{143}Nd/^{144}Nd$	0.512298	0.512404	0.512265	0.512363	0.512155
2σ	0.000011	0.000013	0.000013	0.000014	0.000013
t_{2DM}(Ga)	1.6	1.6	1.5	1.6	1.7
$\varepsilon_{Nd}(t)$	−6.9	−7.1	−6.6	−7.0	−9.0

tends to be Al_2O_3-, and K_2O-poor according to negative correlation of Al_2O_3 and K_2O with SiO_2, perhaps resulted from disappearance of biotite. This is in accord with petrography that the proportion of biotite is low but garnet occupies a large proportion of the accessory minerals. Therefore, MnO-rich garnet could crystallize at the expense of biotite in a highly evolved MnO-rich magma. However, increasing Al in the melt is not necessary due to the metaluminous character of the Erlangmiao granite.

Zircon saturation temperature (690−760 °C) of the Erlangmiao granite, calculated by the geothermometer of initially presented by Watson and Harrison (1983) and revised by Miller et al. (2003), provides a minimum crystallization temperature of the granite because the evolved granitic melt was invariably saturated in zircon (Miller et al., 2003). The 'spessartine inverse bell-shaped profile' of garnet from granite was caused by diffusion above 700 °C (Dahlquist et al., 2007) and is evidence of crystal growth under conditions of falling temperature (Allan and Clarke, 1981). This is the case for the Erlangmiao zoned garnet, which supports the crystallization temperature from zircon saturation geothermometer. Garnet generally crystallizes from high-silica granite under very low-pressure conditions, estimated as low as 2−3 kbar by Speer and Becker (1992) and even as low as 1 kbar by Clemens and Wall (1981). As for the Erlangmiao granite, although no precise geobarometry can be used, field features indicate that it was emplaced at a shallow crustal level and thus formed under low-*p* conditions.

8.2. Petrogenesis

8.2.1. Classification of the Erlangmiao granite

Granitoids are genetically divided into I-, S-, M-, and A-types. A-type granites, firstly defined by Loiselle and Wones (1979), were generally emplaced at a shallow crustal level and may vary in lithology from syenite to metaluminous and peralkaline granite. These rocks are commonly low in Al_2O_3, CaO, H_2O and high in alkalis, and FeO_t/MgO and TiO_2/MgO ratios. Their REE contents (except Eu), Ga, Zr, Nb, and Ta are usually high, while their Ba, Sr, and Eu contents are low, with high zircon saturation temperature (Collins et al., 1982; Clemens et al., 1986; Whalen et al., 1987; Eby, 1990, 1992; Creaser et al., 1991). They were mostly formed under H_2O undersaturated (Clemens et al., 1986; Dall'Agnol et al., 1999; Klimm et al., 2003) and oxidized (Dall'Agnol and de Oliveira, 2007) conditions in extensional environments. Classification of highly evolved granite may not be confidently done by the above diagnostic elements, such as distinguishing metaluminous A-type granites from highly fractionated I-type granites, especially while lack of a less evolved association within pluton (King et al., 1997).

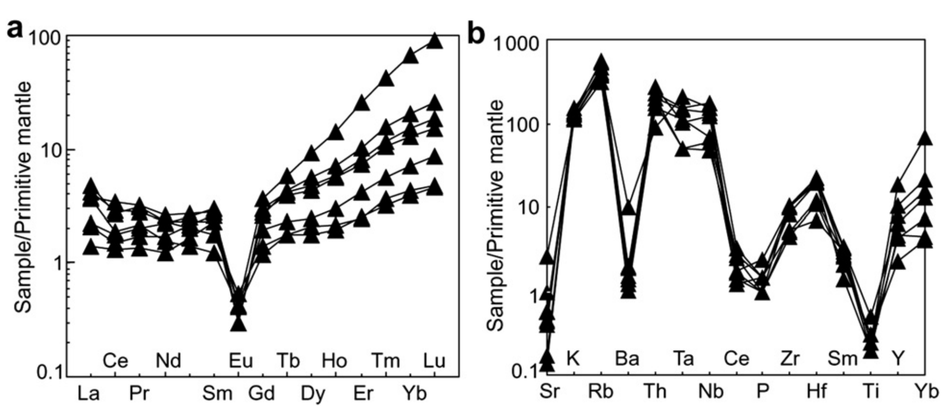

Figure 4 a: Primitive mantle-normalized REE patterns, and b: spider diagrams of the Erlangmiao granite. Normalized data from Wood et al. (1979, 1980).

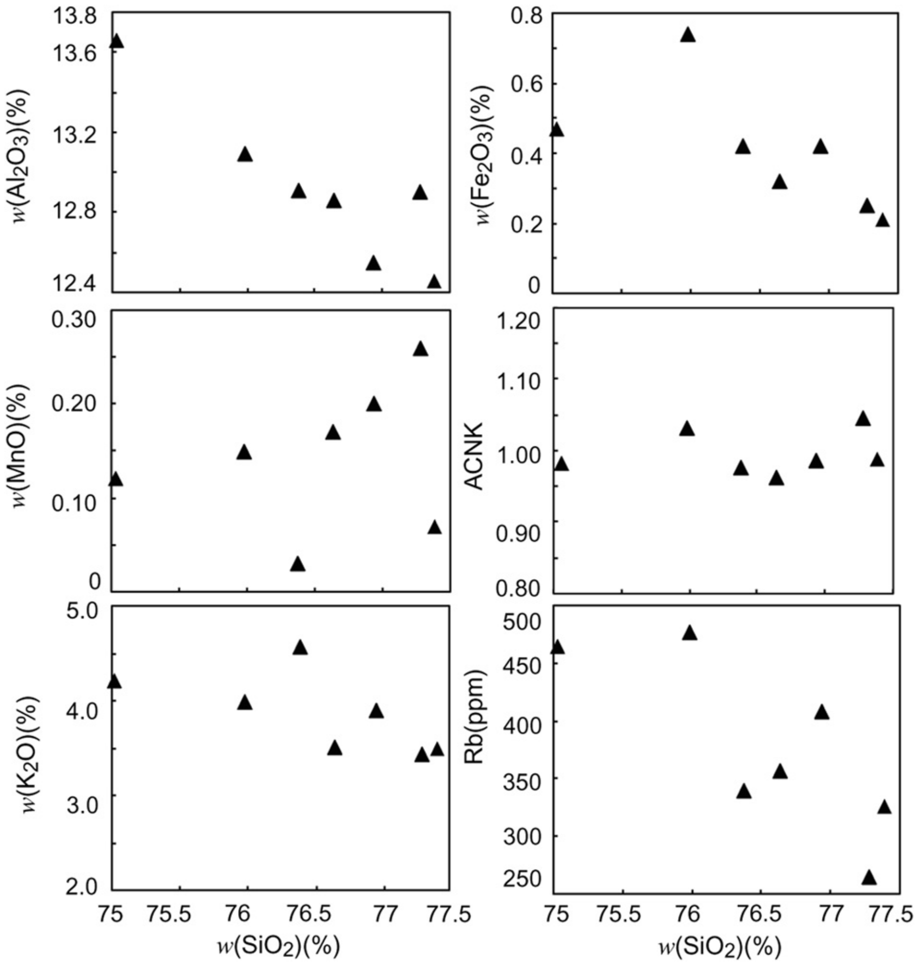

Figure 5 Harker diagrams for the Erlangmiao granite.

Though containing accessory garnet, the Erlangmiao granite is obviously distinct with typical garnet-bearing S-type because of its relative low ACNK ratios and P_2O_5 contents (King et al., 1997, 2001; Zhang et al., 2004b), but is best classified as metaluminous A-type (X.H. Li et al., 2007). The rocks have high alkalis contents and low Al_2O_3 and CaO contents. Their FeO_t/MgO and TiO_2/MgO ratios and Ga, Ta, Nb, Y, and Yb contents are relative high, with Y/Nb < 1.2 (except sample 05DB21-1). This is also evident in discrimination diagrams (Fig. 6) in which all samples plot in the field of A-type granites.

Compositions of magmatic garnet from granites might provide information about the classification of their host. We demonstrate this by examining reported major elements of magmatic garnet from various granites in the literature and the results are

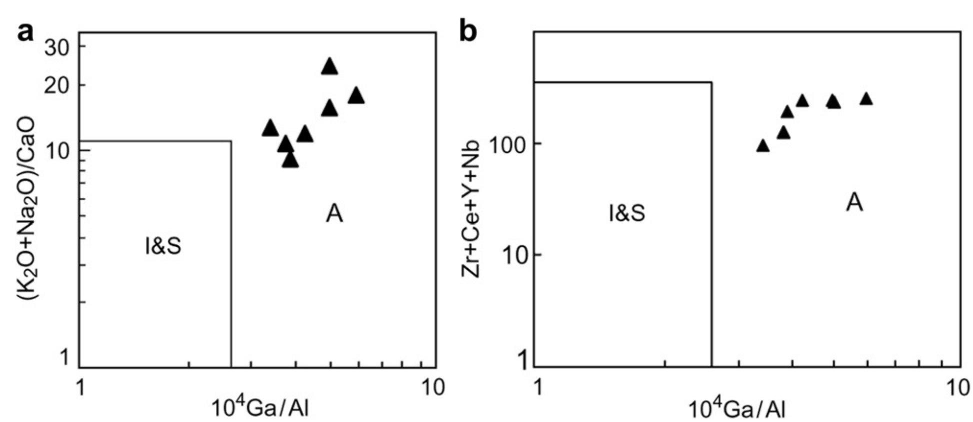

Figure 6 A-type granites discrimiation diagrams for the Erlangmiao granite after Whalen et al. (1987). A, I, and S refer to A-type, I-type, and S-type granite.

summarized in Fig. 7. It is evident that garnet from A-type granites tends to have higher MnO, and lower FeO and MgO contents, whereas garnet from S-type granites has a variable and wide range of MnO, FeO, and MgO contents, although there is a partial overlap. The Erlangmiao garnet is distributed within the area of A-type granites (Fig. 7), confirming the metaluminous A-type attribute of its host.

8.2.2. Magmatic sources

Several hypotheses have been proposed to interpret the genesis of A-type granites (see reviews in Martin, 2006 and Bonin, 2007): (1) fractional crystallization of a mantle-derived mafic magma with or without crustal contamination, (2) crustal rocks fenitized by mantle-derived fluids, (3) remelting of precursor granites or high-grade metasedimentary rocks that underwent an earlier melting event, and (4) melting of calc-alkaline I-type tonalites and granodiorites or hornblende- and biotite-bearing granites in the crust. Though model (4) is still debated, we think that the Erlangmiao metaluminous A-type granite might have originated from partial melting of granitic rocks in the crust based on the following two reasons.

Firstly, Model (4) can illuminate the characteristics of metaluminous A-type granite (Patiño Douce, 1997) while the other three models have their limitations. Model (1) can interpret the origin of peralkaline granites (Peccerillo et al., 2003). Model (2) could explain well the anorogenic igneous suites including carbonatite, nephelinite, phonolite, syenite, and granite (Woolley, 1987; Martin, 2006). Model (3) cannot explain some geochemical signatures of A-type granites such as low Al_2O_3, CaO and high K_2O, SiO_2 (Patiño Douce, 1997).

Secondly, Early Cretaceous migmatization pervasively affected the Paleoproterozoic granitic gneisses in the region, showing a genetic relationship between the Paleoproterozoic granitic gneisses and Early Cretaceous granites. This can be established using the Nd isotope data. The Paleoproterozoic granitic gneisses have nearly the same ε_{Nd} (120 Ma) values (Zhang et al., 1994) as the Early Cretaceous granites in the region (Fig. 8) (Zhou et al., 2008) and Nd model ages (∼2.0 Ga) of the Early Cretaceous granites and the formation age of the Paleoproterozoic granitic gneisses are also similar, whereas the ε_{Nd} (120 Ma) values of the Erlangmiao granite (−6.6 to −9.0) are less negative and its Nd model ages (1.5−1.7 Ga) are younger. Considering the gradually increased role of the asthenosphere during the Early Cretaceous in the Qinling−Dabie region (Chen et al., 2010), we infer that partial melting of the Paleoproterozoic granitic gneisses formed Early Cretaceous granites, subsequently, with participation of depleted mantle, continuous partial melting possibly produced the Erlangmiao granite.

8.2.3. Fractional crystallization

The Erlangmiao granite contains almost 99% felsic minerals, together with high SiO_2, low FeO, Fe_2O_3, MgO, Eu, Sr, Ba, P, and Ti contents, demonstrating that it is highly evolved. Petrographical evidence and the very low MgO content indicate separation of biotite. Strong Eu depletion requires extensive fractionation of plagioclase and/or K-feldspar. It could also be caused by fluid-melt interaction process in highly evolved magmas. The REE tetrad effect will arise if fluids interact with the fractionated granitic melt (Wu et al., 2004). The tetrad REE patterns are not observed in the Erlangmiao granite and their TE1, 3 are mostly lesser than 1.0, which indicates that fluid-melt interaction is insignificant. Fractionation of plagioclase would result in unity of ACNK, increasing NK/A molar $((Na_2O + K_2O)/Al_2O_3)$ ratios and negative Sr-Eu anomalies, while separation of K-feldspar would lead to increasing Na_2O/K_2O ratios and negative Eu-Ba anomalies (Wu et al., 2003). Fractionation of K-feldspar usually follows that of plagioclase (Couch, 2003). Europium, Sr, and Ba of the Erlangmiao granite are negative anomaly, ACNK ratios tend to unity and Na_2O/K_2O ratios increase while K_2O, Na_2O decrease with increasing SiO_2 (Fig. 5), which favors fractional crystallization of plagioclase and K-feldspar. Low ΣREE contents of the Erlangmiao granite suggest separation of REE-rich minerals and low Zr, P, and Ti contents further indicate fractional crystallization

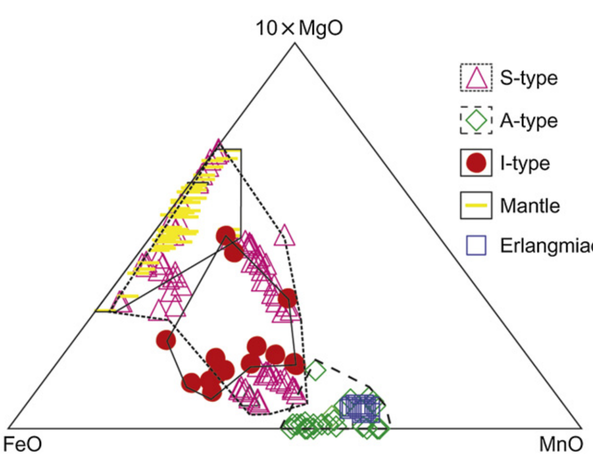

Figure 7 FeO-10× MgO-MnO triangular diagram of garnet from various genetic granites. I-type, S-type, A-type, and Mantle represent garnet from I-type granites, S-type granites, A-type granites, and igneous rocks originating from mantle. Major elements of garnet are from: I-type granites, Wu et al. (2004) and Yu et al. (2004); S-type granites, Plank (1987), Kebede et al. (2001), Jung et al. (2001), Jung and Hellebrand (2006), and Dahlquist et al. (2007); A-type granites, du Bray (1988), Wu et al. (2004), Wang et al. (2003), and Yu et al. (2005); igneous rocks originating from mantle, Kawabata and Takafuji (2005), Harangi et al. (2001), and Chen and Zhao (1991).

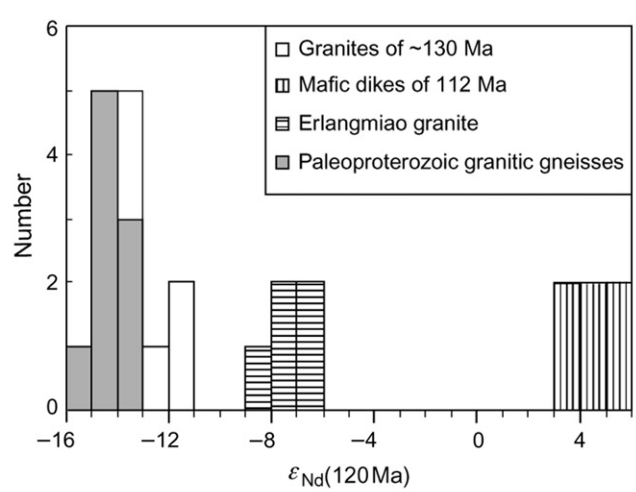

Figure 8 Histogram of ε_{Nd} (120 Ma) values from the Erlangmiao granite, the Paleoproterozoic granitic gneisses (Zhang et al., 1994 and our two unpublished data), the Early Cretaceous granites (Zhou et al., 2008), and the mafic dikes (Chen et al., 2010).

of zircon, apatite, and ilmenite. Fractionation makes the characteristics of the Erlangmiao granite depart from typical metaluminous A-type granites to some extent (King et al., 2001; Xie et al., 2006), such as low FeO, Fe_2O_3, MgO, Zr, and Nb contents.

9. Conclusions

(1) The Erlangmiao garnet-bearing syenogranite in the East Qinling Orogen contains almost 99% felsic minerals and was emplaced at a shallow crustal level. The garnet, as the dominant accessory mineral, is rich in FeO and MnO and crystallized at the expense of biotite from MnO-rich granitic magma.

(2) Petrography, garnet chemistry and whole rock geochemistry suggest that the Erlangmiao granite is a highly evolved metaluminous A-type that underwent extensive fractionation of biotite, plagioclase, K-feldspar, zircon, apatite, and ilmenite. The initial magma originated from partial melting of the Paleoprotozoic granitic gneissic basement, with participation of depleted mantle in an extensional environment.

Acknowledgments

This study was financially supported by the Key International S & T Cooperation Project (No. 2007DFA21230) of the Ministry of Science and Technology, the Natural Science Foundation of China (No. 40521001, 40334037, and 40903017), Nature Science Foundation of Hubei Province (No. 2009CDA004), and the Ministry of Education of China and the State Administration of Foreign Expert Affairs of China (No. B07039).

References

Abbott, R.N., 1981. AFM liquidus projections for granitic magmas, with special reference to hornblende, biotite and garnet. Canadian Mineralogist 19, 103–110.

Allan, B.D., Clarke, D.B., 1981. Occurrence and origin of garnets in the South Mountain batholith, Nova Scotia. Canadian Mineralogist 19, 19–24.

Aydar, E., Gourgaud, A., 2002. Garnet-bearing basalts: an example from Mt. Hasan, Central Anatolia, Turkey. Mineralogy and Petrology 75, 185–201.

Barbarin, B., 1996. Genesis of the two main types of peraluminous granitoid. Geology 24, 295–298.

Barbarin, B., 1999. A review of the relationships between granitoid types, their origins and their geodynamic environment. Lithos 46, 605–626.

Barovich, K.M., Patchett, P.J., 1992. Behavior of isotopic systematics during deformation and metamorphism – a Hf, Nd and Sr isotopic study of mylonitized granite. Contributions to Mineralogy and Petrology 109, 386–393.

BGMRHP, 1989. Regional Geology of Henan Province. Geological Publishing House, Beijing, 1–234 pp. (in Chinese).

Bialek, D., 1999. Chemical changes associated with deformation of granites under greenschist facies conditions: the example of the Zawidow Granodiorite (SE Lusatian Granodiorite Complex, Poland). Tectonophysics 303, 251–261.

Bonin, B., 2007. A-type granites and related rocks: evolution of a concept, problems and prospects. Lithos 97, 1–29.

Chappell, B.W., White, A.J.R., 1974. Two contrasting granite types. Pacific Geology 8, 173–174.

Chen, F.K., Hegner, E., Todt, W., 2000. Zircon ages and Nd isotopic and chemical compositions of orthogneisses from the Black Forest, Germany: evidence for a Cambrian magmatic arc. International Journal of Earth Sciences 88, 791–802.

Chen, L., Ma, C.Q., Zhang, J.Y., Mason, R., Zhang, C., 2010. Mafic dykes derived from Early Cretaceous depleted mantle beneath the Dabie orogenic belt: implications for changing lithosphere mantle beneath eastern China. Geological Journal 45, 1–11.

Chen, X.H., Zhao, Y.Q., 1991. Characteristics, genesis and petrogenic significance of garnet phenocrysts in acid lavas from the Xiling mining area. Geochimica 1, 33–39 (in Chinese with English abstract).

Clemens, J.D., 2003. S-type granitic magmas – petrogenetic issues, models and evidence. Earth-Science Reviews 61, 1–18.

Clemens, J.D., Wall, V.J., 1981. Origin and crystallization of some peraluminous (S-type) granitic magmas. Canadian Mineralogist 10, 111–131.

Clemens, J.D., Wall, V.J., 1984. Origin and evolution of a peraluminous silicic ignimbrite suite: the Violet Town volcanics. Contributions to Mineralogy and Petrology 88, 354.

Clemens, J.D., Holloway, J.R., White, A., 1986. Origin of an A-type granite – experimental constraints. American Mineralogist 71, 317–324.

Collins, W.J., Beams, S.D., White, A.J.R., Chappell, B.W., 1982. Nature and origin of A-type granites with particular reference to southeastern Australia. Contributions to Mineralogy and Petrology 80, 189–200.

Couch, S., 2003. Experimental investigation of crystallization kinetics in a haplogranite system. American Mineralogist 88, 1471–1485.

Creaser, R.A., Price, R.C., Wormald, R.J., 1991. A-type granites revisited – assessment of a residual-source model. Geology 19, 163–166.

Dahlquist, J.A., Galindo, C., Pankhurst, R.J., Rapela, C.W., Alasino, P.H., Saavedra, J., Fanning, C.M., 2007. Magmatic evolution of the Penon Rosado granite: petrogenesis of garnet-bearing granitoids. Lithos 95, 177–207.

Dall'Agnol, R., de Oliveira, D.C., 2007. Oxidized, magnetite-series, rapakivi-type granites of Carajas, Brazil: implications for classification and petrogenesis of A-type granites. Lithos 93, 215–233.

Dall'Agnol, R., Scaillet, B., Pichavant, M., 1999. An experimental study of a Lower Proterozoic A-type granite from the eastern Amazonian craton, Brazil. Journal of Petrology 40, 1673–1698.

Day, R.A., Green, T.H., Smith, I., 1992. The origin and significance of garnet phenocrysts and garnet-bearing xenoliths in Miocene calc-alkaline volcanics from Northland, New-Zealand. Journal of Petrology 33, 125–161.

Deer, W.A., Howie, R.A., Zussman, J., 1992. An Introduction to the Rock Forming Minerals, Second Longman ed. Longman, London, 696 pp.

Droop, G., 1987. A general equation for estimating Fe^{3+} concentrations in ferromagnesian silicates and oxides from microprobe analyses, using stoichiometric criteria. Mineralogical Magazine 51, 431–435.

du Bray, E.A., 1988. Garnet compositions and their use as indicators of peraluminous granitoid petrogenesis – southeastern Arabian Shield. Contributions to Mineralogy and Petrology 100, 205–212.

Eby, G.N., 1990. The A-type granitoids – a review of their occurrence and chemical characteristics and speculations on their petrogenesis. Lithos 26, 115–134.

Eby, G.N., 1992. Chemical subdivision of the A-type granitoids: petrogenetic and tectonic implications. Geology 20, 641–644.

Embey-Isztin, A., Noske-Fazekas, G., Kurat, G., Brandstatter, F., 1985. Genesis of garnets in some magmatic rocks from Hungary. Tschermaks Mineralogische und Petrographische Mitteilungen 34, 49–66.

Gao, S., Zhang, B.R., Xie, Q.L., Gu, X.M., Ouyang, J.P., Wang, D.P., Gao, C.G., 1991. Average chemical-compositions of post-Archean sedimentary and volcanic-rocks from the Qinling orogenic belt and its adjacent North China and Yangtze cratons. Chemical Geology 92, 261–282.

Gilbert, J.S., Rogers, N.W., 1989. The significance of garnet in the Permo-Carboniferous volcanic-rocks of the Pyrenees. Journal of the Geological Society 146, 477–490.

Green, T.H., 1977. Garnet in silicic liquids and its possible use as a p–T indicator. Contributions to Mineralogy and Petrology 65, 59.

Green, T.H., Ringwood, A.E., 1968. Origin of garnet phenocrysts in calc-alkaline rocks. Contributions to Mineralogy and Petrology 18, 163.

Hamer, R.D., Moyes, A.B., 1982. Composition and origin of garnet from the Antarctic Peninsula volcanic group of Trinity Peninsula. Journal of the Geological Society 139, 713–720.

Harangi, S., Downes, H., Kosa, L., Szabo, C., Thirlwall, M.F., Mason, P.R.D., Mattey, D., 2001. Almandine garnet in calc-alkaline volcanic rocks of the Northern Pannonian Basin (Eastern-Central Europe): geochemistry, petrogenesis and geodynamic implications. Journal of Petrology 42, 1813–1843.

Hogan, J.P., 1996. Insight from igneous reaction space: a holistic approach to granite crystallization. Transactions of the Royal Society of Edinburgh: Earth Sciences 87, 147–157.

Jung, S., Hellebrand, E., 2006. Trace element fractionation during high-grade metamorphism and crustal melting-constraints from ion microprobe data of metapelitic, migmatitic and igneous garnets and implications for Sm–Nd garnet chronology. Lithos 87, 193–213.

Jung, S., Mezger, K., Hoernes, S., 2001. Trace element and isotopic (Sr, Nd, Pb, O) arguments for a mid-crustal origin of Pan-African garnet-bearing S-type granites from the Damara orogen (Namibia). Precambrian Research 110, 325–355.

Kawabata, H., Takafuji, N., 2005. Origin of garnet crystals in calc-alkaline volcanic rocks from the Setouchi volcanic belt, Japan. Mineralogical Magazine 69, 951–971.

Kebede, T., Koeberl, C., Koller, F., 2001. Magmatic evolution of the Suquii-Wagaa garnet-bearing two-mica granite, Wallagga area, western Ethiopia. Journal of African Earth Sciences 32, 193–221.

Kemp, A., Hawkesworth, C.J., Foster, G.L., Paterson, B.A., Woodhead, J.D., Hergt, J.M., Gray, C.M., Whitehouse, M.J., 2007. Magmatic and crustal differentiation history of granitic rocks from Hf-O isotopes in zircon. Science 315, 980–983.

Kerrich, R., Allison, I., Barnett, R.L., Moss, S., Starkey, J., 1980. Microstructural and chemical transformations accompanying deformation of granite in a shear zone at Miéville, Switzerland; with implications for stress corrosion cracking and superplastic flow. Contributions to Mineralogy and Petrology 73, 221.

King, P.L., Chappell, B.W., Allen, C.M., White, A., 2001. Are A-type granites the high-temperature felsic granites? Evidence from fractionated granites of the Wangrah Suite. Australian Journal of Earth Sciences 48, 501–514.

King, P.L., White, A., Chappell, B.W., Allen, C.M., 1997. Characterization and origin of aluminous A-type granites from the Lachlan Fold Belt, Southeastern Australia. Journal of Petrology 38, 371–391.

Klimm, K., Holtz, F., Johannes, W., King, P.L., 2003. Fractionation of metaluminous A-type granites: an experimental study of the Wangrah Suite, Lachlan Fold Belt, Australia. Precambrian Research 124, 327–341.

Lackey, J.S., Valley, J.W., Hinke, H.J., 2006. Deciphering the source and contamination history of peraluminous magmas using italic type^{18}O of accessory minerals: examples from garnet-bearing plutons of the Sierra Nevada batholith. Contributions to Mineralogy and Petrology 151, 20–44.

Li, S.Z., Kusky, T.M., Wang, L., Zhang, G.W., Lai, S.C., Liu, X.C., Dong, S.W., Zhao, G.C., 2007. Collision leading to multiple-stage large-scale extrusion in the Qinling orogen: insights from the Mianlue suture. Gondwana Research 12, 121–143.

Li, X.H., 1996. A discussion on the model and isochron ages of Sm–Nd isotopic systematics: suitability and limitation. Scientia Geological Sinica 31, 97–104 (in Chinese with English abstract).

Li, X.H., Li, Z.X., Li, W.X., Liu, Y., Yuan, C., Wei, G.J., Qi, C.S., 2007. U-Pb zircon, geochemical and Sr-Nd-Hf isotopic constraints on age and origin of Jurassic I- and A-type granites from central Guangdong, SE China: a major igneous event in response to foundering of a subducted flat-slab? Lithos 96, 186–204.

Li, X.Z., Yan, Z., Lu, X.X., 1993. Granitioids in Qinling-Dabieshan. Geological Publishing House, Beijing, 1–53 pp. (in Chinese).

Loiselle, M.C., Wones, D.R., 1979. Characteristics and origin of anorogenic granites. Geological Society of America Abstracts with Programs 11, 468.

Martin, R.F., 2006. A-type granites of crustal origin ultimately result from open-system fenitization-type reactions in an extensional environment. Lithos 91, 125–136.

Miller, C.F., Stoddard, E.F., 1981. The role of manganese in the paragenesis of magmatic garnet: an example from the Old Woman-Piute Range, California. Journal of Geology 89, 233–246.

Miller, C.F., Mcdowell, S.M., Mapes, R.W., 2003. Hot and cold granites? Implications of zircon saturation temperatures and preservation of inheritance. Geology 31, 529–532.

Mirnejad, H., Blourian, G.H., Kheirkhah, M., Akrami, M.A., Tutti, F., 2008. Garnet-bearing rhyolite from Deh-Salm area, Lut block, Eastern Iran: anatexis of deep crustal rocks. Mineralogy and Petrology 94, 259–269.

Patiño Douce, A., 1997. Generation of metaluminous A-type granites by low-pressure melting of calc-alkaline granitoids. Geology 25, 743–746.

Patranabis-Deb, S., Schieber, J., Basu, A., 2009. Almandine garnet phenocrysts in a similar to 1 Ga rhyolitic tuff from central India. Geological Magazine 146, 133–143.

Peccerillo, A., Barberio, M.R., Yirgu, G., Ayalew, D., Barbieri, M., Wu, T.W., 2003. Relationships between mafic and peralkaline acid magmatism in continental rift settings: a petrological, geochemical and isotopic study of the Gedemsa volcano, central Ethiopian rift. Journal of Petrology 44, 2003–2032.

Plank, T., 1987. Magmatic garnets from the Cardigan pluton and the Acadian thermal event in southwest New-Hampshire. American Mineralogist 72, 681–688.

Ratschbacher, L., Hacker, B.R., Calvert, A., Webb, L.E., Grimmer, J.C., Mcwilliams, M.O., Ireland, T., Dong, S., Hu, J., 2003. Tectonics of the Qinling (central China): tectonostratigraphy, geochronology, and deformation history. Tectonophysics 366, 1–53.

René, M., Stelling, J., 2007. Garnet-bearing granite from the Třebíč pluton, Bohemian massif (Czech Republic). Mineralogy and Petrology 91, 55–69.

Speer, J.A., Becker, S.W., 1992. Evolution of magmatic and subsolidus AFM mineral assemblages in granitoid rocks – biotite, muscovite, and garnet in the Cuffytown Creek, pluton, South-Carolina. American Mineralogist 77, 821–833.

Stevens, G., Villaros, A., Moyen, J.F., 2007. Selective peritectic garnet entrainment as the origin of geochemical diversity in S-type granites. Geology 35, 9–12.

Stone, M., 1988. The significance of almandine garnets in the Lundy and Dartmoor granites. Mineralogical Magazine 52, 651–658.

Sylvester, P.J., 1998. Post-collisional strongly peraluminous granites. Lithos 45, 29–44.

Tseng, C.Y., Yang, H.J., Yang, H.Y., Liu, D.Y., Wu, C.L., Cheng, C.K., Chen, C.H., Ker, C.M., 2009. Continuity of the North Qilian and North Qinling orogenic belts, Central Orogenic System of China: evidence from newly discovered paleozoic adakitic rocks. Gondwana Research 16, 285–293.

Villaros, A., Stevens, G., Buick, I.S., 2009. Tracking S-type granite from source to emplacement: clues from garnet in the Cape granite suite. Lithos 112, 217–235.

Wang, R.C., Hu, H., Zhang, A.C., Xu, S.J., Wang, D.Z., 2003. Yttrium zoning in garnet from the Xihuashan granitic complex and its petrological implications. Chinese Science Bulletin 48, 1611–1615.

Watson, E.B., Harrison, T.M., 1983. Zircon saturation revisited – temperature and composition effects in a variety of crustal magma types. Earth and Planetary Science Letters 64, 295–304.

Whalen, J.B., Currie, K.L., Chappell, B.W., 1987. A-type granites – geochemical characteristics, discrimination and petrogenesis. Contributions to Mineralogy and Petrology 95, 407–419.

White, A., Clemens, J.D., Holloway, J.R., Silver, L.T., Chappell, B.W., Wall, V.J., 1986. S-type granites and their probable absence in southwestern North-America. Geology 14, 115–118.

Whitworth, M.P., 1992. Petrogenetic implications of garnets associated with lithium pegmatites from SE Ireland. Mineralogical Magazine 56, 75–83.

Wood, D.A., Joron, J.L., Treuil, M., Norry, M., Tarney, J., 1979. Elemental and Sr isotope variations in basic lavas from Iceland and the surrounding ocean floor. Contributions to Mineralogy and Petrology 70, 319–339.

Wood, D.A., Tarney, J., Weaver, B.L., 1980. Trace element variations in Atlantic Ocean basalts and Proterozoic dykes from northwest Scotland:

their bearing upon the nature and geochemical evolution of the upper mantle. Tectonophysics 75, 91−112.

Woolley, A.R., 1987. Lithosphere metasomatism and the petrogenesis of the Chilwa province of alkaline igneous rocks and carbonatites, Malawi. Journal of African Earth Sciences 6, 891−898.

Wu, F.Y., Jahn, B.M., Wilde, S.A., Lo, C.H., Yui, T.F., Lin, Q., Ge, W.C., Sun, D.Y., 2003. Highly fractionated I-type granites in NE China (I): geochronology and petrogenesis. Lithos 66, 241−273.

Wu, F.Y., Sun, D.Y., Jahn, B.M., Wilde, S., 2004. A Jurassic garnet-bearing granitic pluton from NE China showing tetrad REE patterns. Journal of Asian Earth Sciences 23, 731−744.

Xiang, H., Zhang, L., Zhong, Z.Q., Santosh, M., Zhou, H.W., Zhang, H.F., Zheng, J.P., Zheng, S., 2011. Ultrahigh-temperature metamorphism and anticlockwise P-T-t path of Paleozoic granulites from North Qinling-Tongbai orogen, central China. Gondwana Research. doi: 10.1016/j.gr.2011.07.002.

Xie, L., Wang, R.C., Wang, D.Z., Qiu, J.S., 2006. A survey of accessory mineral assemblages in peralkaline and more aluminous A-type granites of the southeast coastal area of China. Mineralogical Magazine 70, 709−729.

Yu, J.H., Zhao, L., Zhou, X., 2004. Mineralogical characteristics and origin of garnet-bearing I-type granitoids in southeastern Fujian province. Geological Journal of China Universities 10, 364−377 (in Chinese with English abstract).

Yu, J.H., Zhou, X.M., Zhao, L., Jiang, S.Y., Wang, L.J., Lang, H.F., 2005. Mantle-crust interaction generating the Wuping granites; evidenced from Sr-Nd-Hf-U-Pb isotopes. Acta Petrologica Sinica 21, 651−664 (in Chinese with English abstract).

Yuan, C., Sun, M., Xiao, W.J., Wilde, S., Li, X.H., Liu, X.H., Long, X.P., Xia, X.P., Ye, K., Li, J.L., 2009. Garnet-bearing tonalitic porphyry from East Kunlun, northeast Tibetan Plateau: implications for adakite and magmas from the mash zone. International Journal of Earth Sciences 98, 1489−1510.

Zhang, C.L., Zhang, G.W., Liu, S., Wang, S.J., Zhou, D.W., Liu, L., 2004a. Zircon LA-ICPMS ages of metamorphosed volcano-sedimentary rocks from the Kuanping Group in the East Qinling. In: 2004’s National Symposium on Petrology and Geodynamics, pp. 355−358 (in Chinese).

Zhang, G.W., Meng, Q.G., Yu, Z.P., Sun, Y., Zhou, D.W., Guo, A.L., 1996. Orogenesis and dynamics of the Qinling orogen. Science in China Series D-Earth Sciences 39, 225−234.

Zhang, H.F., Harris, N., Parrish, R., Kelley, S., Zhang, L., Rogers, N., Argles, T., King, J., 2004b. Causes and consequences of protracted melting of the mid-crust exposed in the North Himalayan antiform. Earth and Planetary Science Letters 228, 195−212.

Zhang, Z.Q., Liu, D.Y., Fu, G.M., 1994. Isotopic Geochronology Research of the Metamorphic Stratum in the North Qinling. Geological Publishing House, Beijing, 1−43 pp. (in Chinese).

Zhou, H.S., Ma, C.Q., Zhang, C., Chen, L., Zhang, J.Y., She, Z.B., 2008. Yanshanian aluminous A-type granitoids in the Chunshui of Biyang, south margin of North China craton: implications from petrology, geochrology and geochemistry. Acta Geologica Sinica 24, 49−64 (in Chinese with English abstract).

Zhou, X., Yu, J.H., 2001. Geochemistry of the granitoids in Mesozoic metamorphic belt of coastal Fujian province. Geochimica 30, 282−292 (in Chinese with English abstract).

Zhu, X.Y., Chen, F.K., Li, S.Q., Yang, Y.Z., Nie, H., Siebel, W., Zhai, M.G., 2011. Crustal evolution of the North Qinling terrain of the Qinling orogen, China: evidence from detrital zircon U-Pb ages and Hf isotopic composition. Gondwana Research 20, 194−204.